Engineering Research Journal
journal homepage: https://erj.journals.ekb.eg/

Prediction of Maximum Dry Density and Angle of Internal Friction Based on Sieve Analysis

Ahmed Mohamed EL-Hanafy[1], Mohammed H AbdelAziz[2], Amany M Ateia[3], Ahmed Elzoghby Elsaied[4,5,*]

[1]National Water Research Center - Construction Research Institute – Egypt
[2]Fayoum University - Faculty of Engineering - Department of Civil Engineering - Egypt
[3] Fayoum University- Faculty of Engineering - Department of Mathematics and Physics – Egypt
[4]National Water Research Center - Construction Research Institute - Egypt
[5]Al-Baha University - Faculty of Engineering - Department of Civil Engineering - Civil Engineering Department - Kingdom of Saudi Arabia
*Corresponding author E-mail: a.elzoghby@bu.edu.sa

Abstract. Grain size distribution (GSD) is widely recognized as a critical index property of soils. This research seeks to derive empirical equations linking maximum dry density and internal friction angle to GSD. It also evaluates the consistency of maximum dry density results from standard and modified proctor compaction tests. The derived relationships provide a quick and pragmatic means to estimate maximum dry density and internal friction angle without extensive laboratory work. The study concentrates on clean sandy soils, some of which contain gravel fractions that vary from 0% to 30%. Equations for maximum dry density were formulated from a dataset of eighty-five compaction tests, while the correlations for internal friction angle were based on the results of ten tests. The findings demonstrate robust relationships between maximum dry density—regardless of whether it comes from the modified or standard proctor method—and sieve data, yielding coefficients of determination (R^2) between 0.58 and 0.97. Higher R^2 values signal a more reliable prediction, confirming that the GSD parameters effectively characterize the compaction behavior of these sandy gravel soils. The best prediction for the internal angle of friction came from combining the particle sizes D_{10}, D_{30}, D_{50}, D_{60}, the sand ratio, and the maximum dry density determined by the modified proctor test, yielding an R^2 of 0.79. On the other hand, the least effective correlation arose when the internal angle of friction was linked solely to the coefficients of uniformity and curvature, along with the maximum dry density from the modified proctor test, resulting in the lowest R^2 value.

Keywords: Predicting Models, Grain Size Analysis, Direct Shear Test, Standard Proctor Test, Modified Proctor Test.

DOI: 10.21608/erj.2025.399920.1260
Received 24 July 2025; Received in revised form 24 July 2025; Accepted 14 August 2025
Available online 01 September 2025

1 Introduction

The availability of top-grade materials for engineering projects has tightened, prompting the industry to embrace a broader palette of soils under the banner of sustainability. Coarse-grained soils have gained favor, since their performance remains relatively stable against moisture fluctuations, a trait the more plastic soils lack. Key to the success of any candidate material is its compaction response, enhancing dry density hinges on tightening the contact between grains and compressing the voids that otherwise lower strength. This process is driven by deliberate external energy, and its efficacy is quantitatively supported by recent studies [1,2]. Soil compaction not only affects the stability and deformation properties of soils, but also their bearing capacity [3,4]. Therefore, it is important to monitor the effectiveness of control of soil compaction by construction operations. Two key parameters that are usually used to assess the compaction performance are the maximum dry density and the optimum moisture content (OMC) [5]. As laboratory determination of these quantities can be laborious and time-consuming there is increasing interest in the use of simplified and time-efficient predictive approaches, especially when the value of experimental data is limited [6]. As Proctor compaction tests (standard and modified) are laborious and it requires number of trials to develop compaction curves, models that can predict compaction parameters as a function of some easily measured soil properties are very important [7]. Recent developments indicate that ML models, especially ensemble methods, could effectively lower the necessity of extensive laboratory studies and improve the effectiveness of soil resource use in construction activities [8]. Precise estimations of OMC and MDD can lead to an increased level of geotechnical design and construction quality, and economic performance. Although the Proctor test is still the conventional and prevailing means of estimating these parameters [9] it has its limitations regarding time, cost, labor, and measuring errors associated with experimental conditions and sample variability [10]. Regression analysis has shown to be a viable statistical estimate of compaction parameters [11-15]. For example, [16] compiled a dataset of 311 sandy and silty-sandy soil samples from the United Arab Emirates and analyzed their soil data. [16] conducted a linear regression on the data, using fines content, liquid limit (LL), plastic limit (PL) and compacting energy to develop a model. They illustrated that, using their model, they could produce nomographs to predict maximum dry density and OMC at 95% confidence level. Additionally, [17] highlighted the use of predictive models in situations where financial or time constraints or early in the design process before extensive field studies are possible. Likewise, [12] investigated 40 finely grained soil samples from Assam, India and found that liquid limit was more correlated to compaction parameters than plastic limit. Their model had an RMSE of 2.1% compared to laboratory values and 7.5% compared to published results. [18] utilized soils located in Ceará, Brazil, which share geological similarities with Bahia (e.g., Barreiras Formation). They modeled compaction properties into nonlinear regression equations to predict compaction properties using index properties such as the Atterberg limits, fines content, and void ratio. They reported mean errors of 2.3% ($R^2 = 0.618$) for maximum dry density, and 8.5% ($R^2 = 0.541$) for OMC but, when comparing these with previous models made by [16] and [18], differences between predicted and laboratory values were significant. In this current experimentation, ten samples were tested for coarse, cohesionless soils to evaluate various combinations of gradation in material composition that could be considered as structural backfill. There will be an additional 150 datasets from previous literature, specifically from [19]. Predictive values will be compared against experimental results, and theoretical models will be constructed to assess consistency and reliability regarding proposed correlations.

2 Materials and Laboratory Testing Program

Sandy samples with gravel fractions between 0 and 30% were used in the present study. Such samples are typically used as structural backfill material below foundations. We carried out several laboratory tests, including grain size distribution, standard and modified Proctor compaction testing, and direct shear box testing.

2.1 Sieve Analysis

The tests were performed according to ASTM D 422- 63 [20]. Table (1) presents the summarized sieve analysis results for the tested samples, while Figure 1 illustrates their corresponding grain size distribution curves.

Table 1 Summary of sieve analysis parameters

Sample Code	% Passed 4.75mm (Sand)	%Retained 4.75mm (Gravel)	D_{10}	Cu	Cc
S0	70.99	29.01	0.25	4.80	0.68
S1	79.26	20.74	0.25	4.80	0.68
S2	95.67	4.33	0.17	2.35	1.07
S3	70.18	29.82	0.19	2.90	0.86
S4	100.00	0.00	1.20	1.75	1.29
S5	76.24	23.76	0.19	2.90	0.86
S6	81.91	18.09	0.19	2.90	0.86
S7	96.97	3.03	0.15	3.24	0.78
S8	95.35	4.65	0.20	2.75	1.11
S9	100.00	0.00	0.15	2.00	0.89

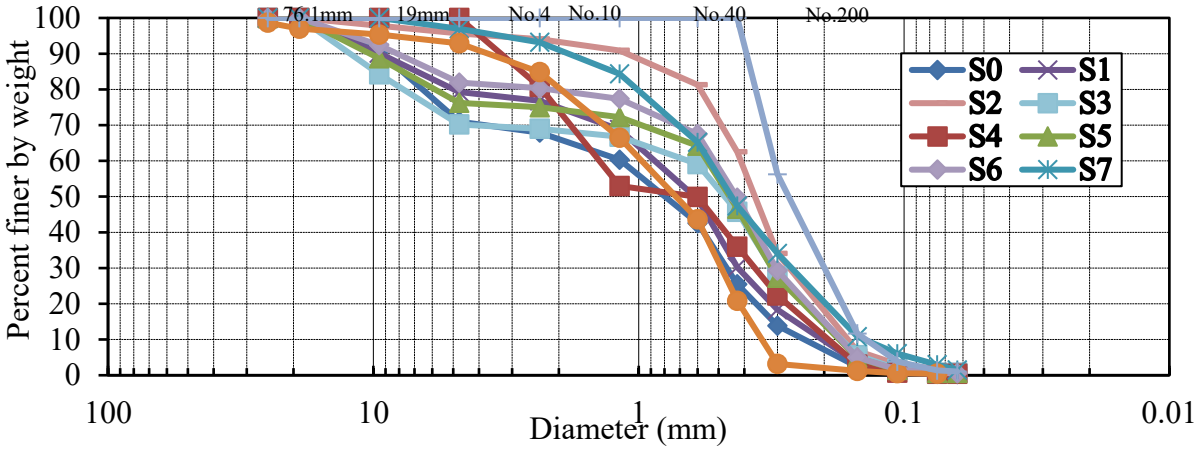

Fig. 1. Grain size distribution analysis

2.2 Compaction Analysis

The compaction curves for the standard and modified proctor compaction tests are shown in Figures 2 and 3, respectively. These tests were performed in compliance with ASTM D1557 [21]. From the compaction tests, it is evident that the modified Proctor maximum dry density is greater than that obtained from Standard Proctor by as much as 3 to 9%. The optimum, the optimum water using Standard Proctor test is up to 2% greater than that obtained using modified Proctor.

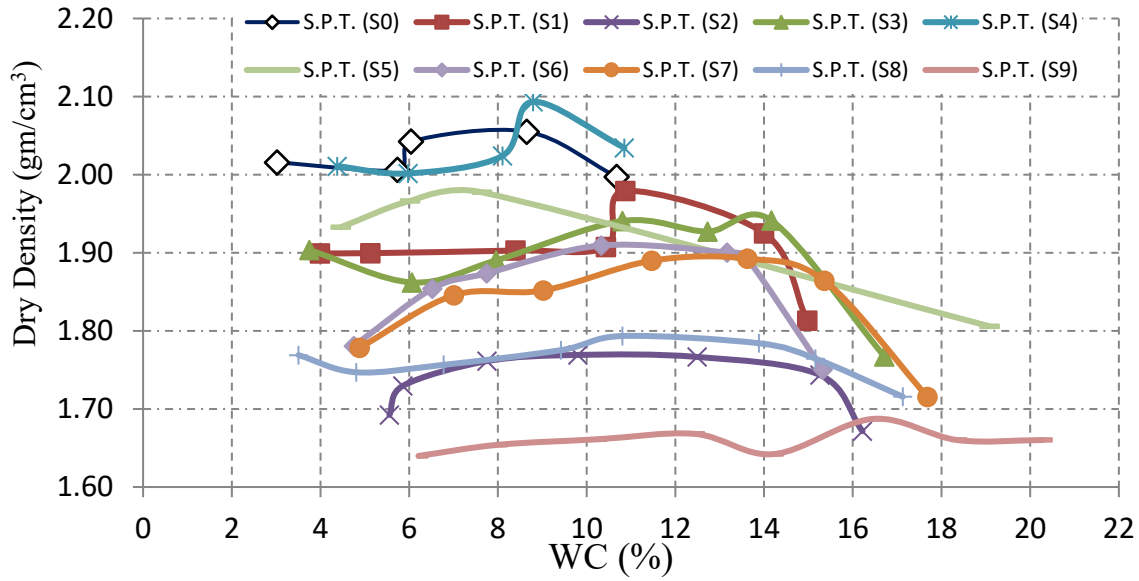

Fig. 2. Standard Proctor Test

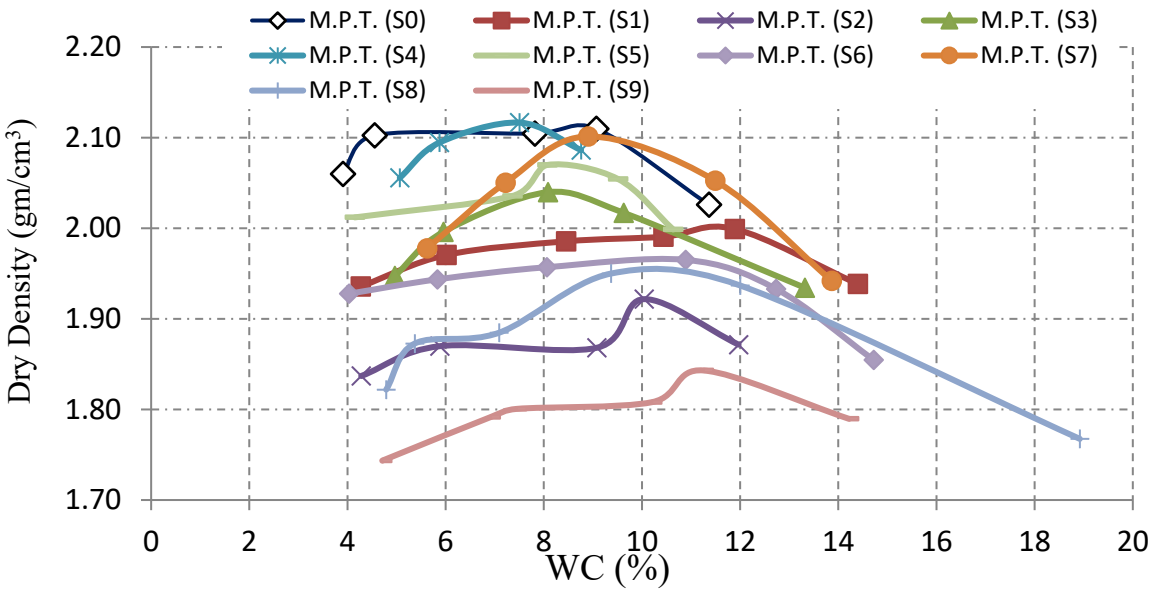

Fig. 3. Modified Proctor Test

2.3 Direct Shear Test

Ten pairs of direct shear tests were performed to assess the shear resistance performance of the sand. All specimens were prepared at their maximum dry unit weights and optimum moisture contents from the standard and modified Proctor compaction tests in accordance with the appropriate standards (ASTM D-698 2010), [22]. Normal stresses of 50, 78, and 106 kPa were applied to all specimens. The shear loading was applied at a rate of 0.12 mm/min. The results of direct shear tests shown in table 2.

Table 2 Results of direct shear tests

Test No.	Angle of internal friction (ϕ)°
S0	41.3
S1	39.58
S2	36.56
S3	40.4
S4	38.7
S5	37.69
S6	39.07
S7	36.3
S8	39.4
S9	28.66

3 Mathematical Analysis

A mathematical analysis was performed to identify relationships between the soil properties of sieve analysis (particle size), maximum dry densities, and shear angles. Multiple linear regression techniques were used to develop empirical correlations between the properties.

3.1 Correlations Between Maximum Dry Density of Standard and Modified Proctor Tests

Equations (1) and (2) demonstrate relationships between maximum dry densities obtained through the standard proctor (SP) and modified proctor (MP) tests. Both equations indicate a relationship between the maximum dry densities obtained from the modified and standard proctor tests, which can either be linear or logarithmic. The R^2 values of equations 1 and 2 are similar. Figures 4 and 5 provide a visual representation of regression plots that compare the actual and predicted maximum dry density values using Equations (1) and (2). Most of the scatter points lie very close to the line of equality and within a ±5% deviation, which demonstrates the correlations indicated by these equations are very strong and valid.

$$\gamma_{max\,(MP)} = 0.1164 + 0.978\,\gamma_{max\,(SP)} \quad \text{Eq 1 } (R^2=0.93)$$

$$\gamma_{max\,(MP)} = 1.737 Ln\,(\gamma_{max\,(SP)}) + 0.86 \quad \text{Eq 2 } (R^2=0.94)$$

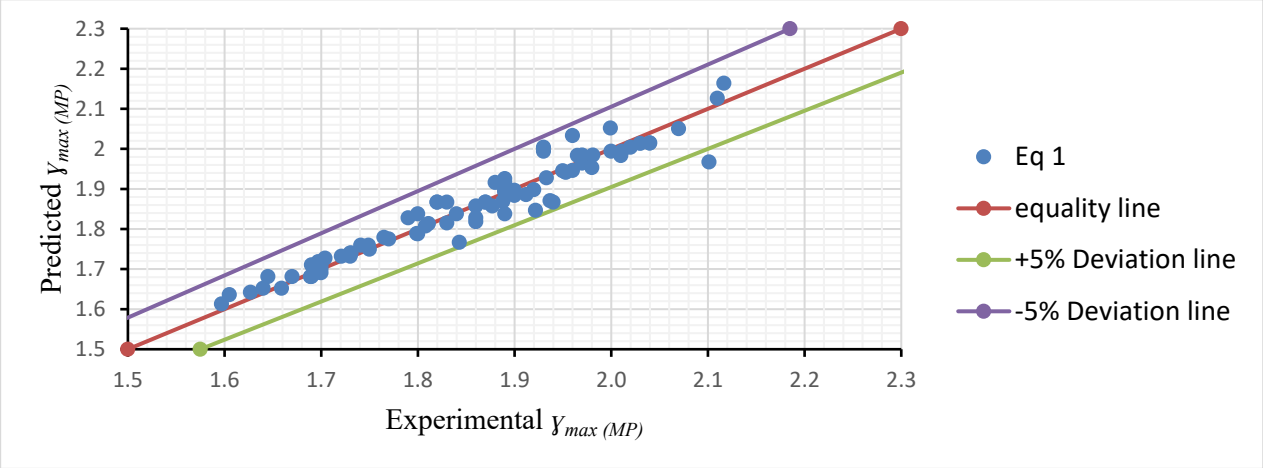

Fig. 4. Regression plot of actual versus predicted maximum dry density values based on equation (1)

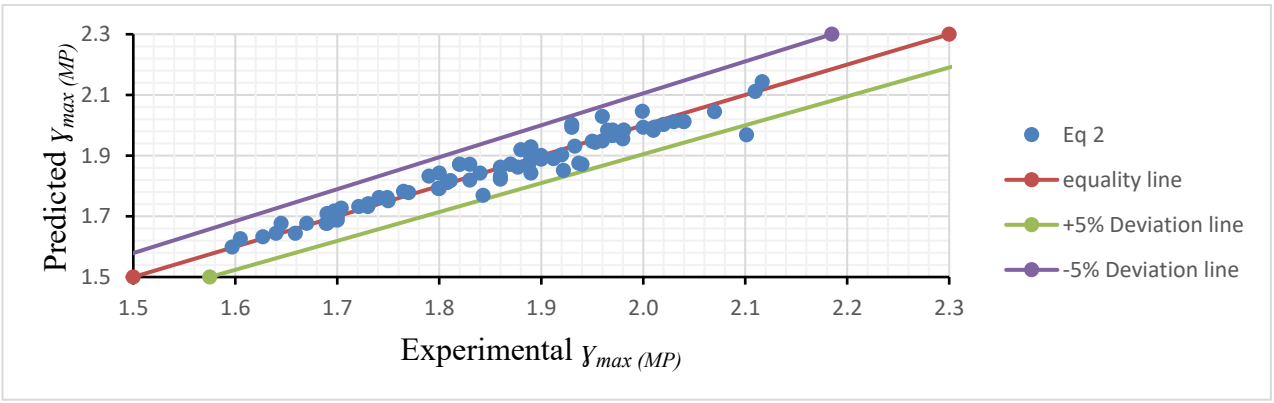

Fig. 5. Regression plot of actual versus predicted maximum dry density values based on equation Eq 2

3.2 Correlations Between Maximum Dry Density of Standard and Modified Proctor Tests

The correlations between maximum dry density and the various sieve analysis parameters of the relationship (C_u), (C_c), effective diameter (D_{10}), and particle diameters corresponding to the values of 30% (D_{30}), 50% (D_{50}) and 60% (D_{60}) by weight were given in the equations (3) and (4). Both equations (3) and (4) resulted in an equal coefficient of determination ($R^2 = 0.58$). The regression plots/figures (example figures, Figure 6 and 7 below) displaying the actual compared to predicted maximum dry densities were based on these values. Most of the reported points from maximum dry density fell within a ±5% deviation, while most scattered points fell outside this limit. The correlations represented in the equations for maximum dry densities can be considered moderate correlations.

$$\gamma_{max\ (MP)} = 1.692 + 0.0496\ Cu - 0.0124\ Cc \quad \text{Eq 3 } (R^2=0.58)$$

$$\gamma_{max\ (MP)} = 1.856 - 0.629\ D10 + 0.0127\ D30 - 0.189\ D50 + 0.303\ D60 \quad \text{Eq 4 } (R^2=0.58)$$

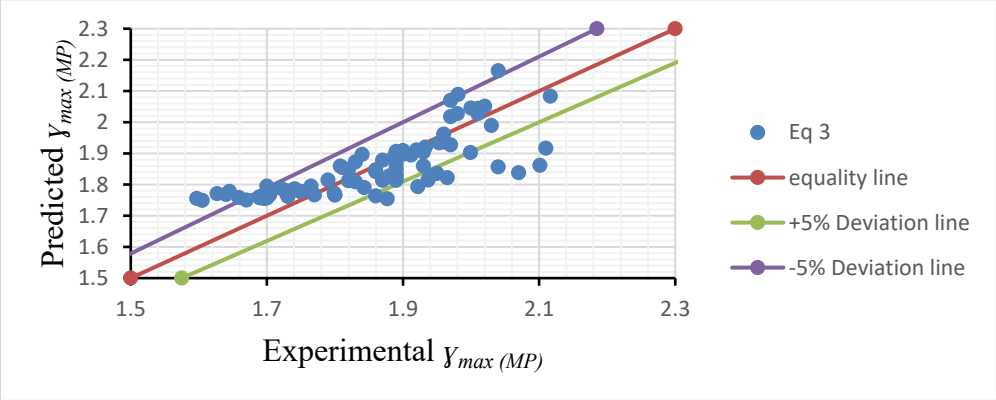

Fig. 6. Regression plot of actual and predicted values of maximum dry densities according to Eq 3

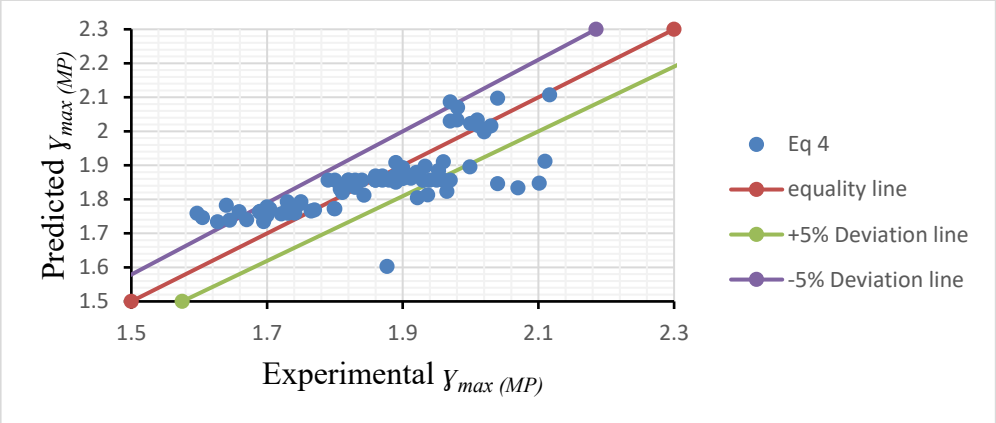

Fig. 7. Regression plot of actual and predicted values of maximum dry densities according to Eq 4

3.3 Correlation Between Maximum Dry Densities from Modified and Standard Proctor Tests and Sieve Analysis Parameters

Equations (5) and (6) show the relationships with the maximum dry densities from modified and standard proctor tests and parameters from the sieving analysis. The prediction capability of these equations is better than the prediction capability of Equations (3) and (4) because the standard proctor maximum dry density was included as one of the input variables. Of the two new equations, Equation (6) showed better prediction performance as shown by the larger coefficient of determination (R^2) when compared to Equation (5). Figures 8 and 9 show that the predicted values strongly correlated with the experimental measured values.

$$\gamma_{max\ (MP)} = 0.167 + 0.0031\ Cu + 0.0026\ Cc + 0.942\gamma_{max\ (SP)} \quad \text{Eq 5 } (R^2=0.93)$$

$$\gamma_{max\ (MP)} = 0.0068 - 0.0903\ D10 - 0.0163\ D30 + 0.1073\ D50 - 0.078\ D60 + 1.057\gamma_{max\ (SP)} \quad \text{Eq 6 } (R^2=0.97)$$

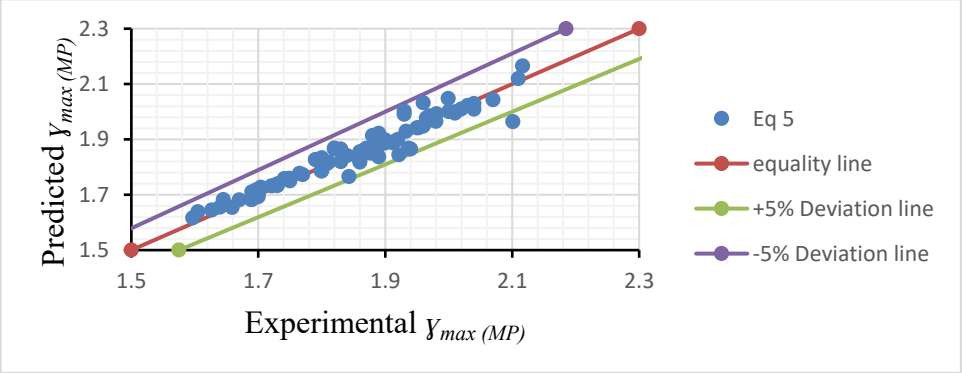

Fig. 8. Regression plot of actual and predicted values of maximum dry densities according to Eq 5

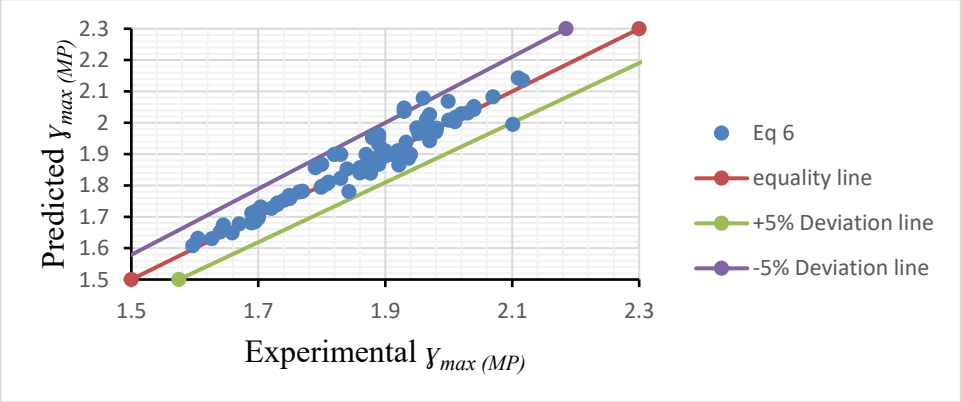

Fig. 9. Regression plot of actual and predicted values of maximum dry densities according to Eq 6

3.4 Prediction of Internal Angle of Friction Based on Sieve Analysis Test

Equations (7), (8), and (9) show the relationships between the internal friction angle (ϕ) and sieve analysis parameters. The experimental values of friction angles obtained from direct shear tests are plotted against the predicted values in Figures 10, 11, and 12. Equation (7) relates the ϕ with size particles D_{10}, D_{30}, D_{50} ,and D_{60}. Equation (9) relates the ϕ to the sand ratio S, while Equation (8) covers both particle sizes (D_{10}, D_{30}, D_{50}, D_{60}), and the sand ratio (S). For each of the equations, the coefficients of determination (R^2) range from 0.57 to 0.73 with Equation (8) providing the most accurate prediction.

$$\phi = 33.37 - 53.65\ D10 + 65.768\ D30 - 3.37\ D50 - 4.958\ D60 \quad \text{Eq 7 } (R^2=0.57)$$

$$\phi = 50.532 - 0.161\ S - 7.821\ D10 + 42.303\ D30 - 16.891\ D50 - 0.847\ D60 \quad \text{Eq 8 } (R^2=0.73)$$

$$\phi = 57.34 - 0.196\ S \quad \text{Eq 9 } (R^2=0.64)$$

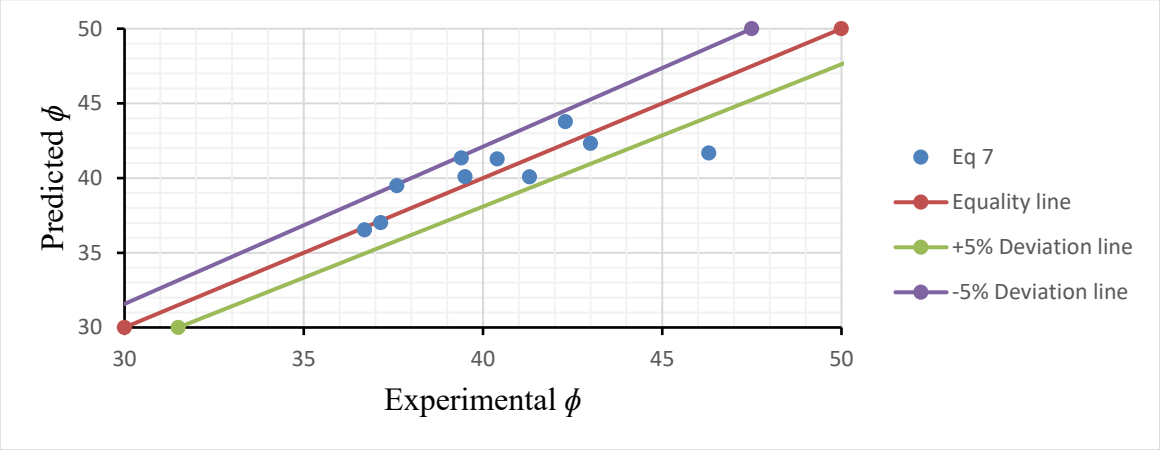

Fig. 10. Regression plot of actual and predicted values of friction angle according to Eq 7

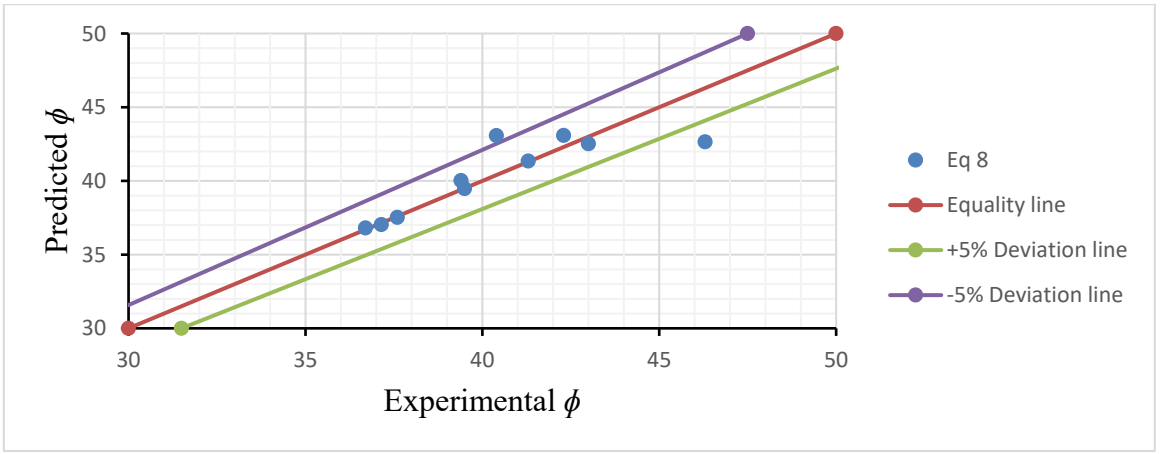

Fig. 11. Regression plot of actual and predicted values of friction angle according to Eq 8

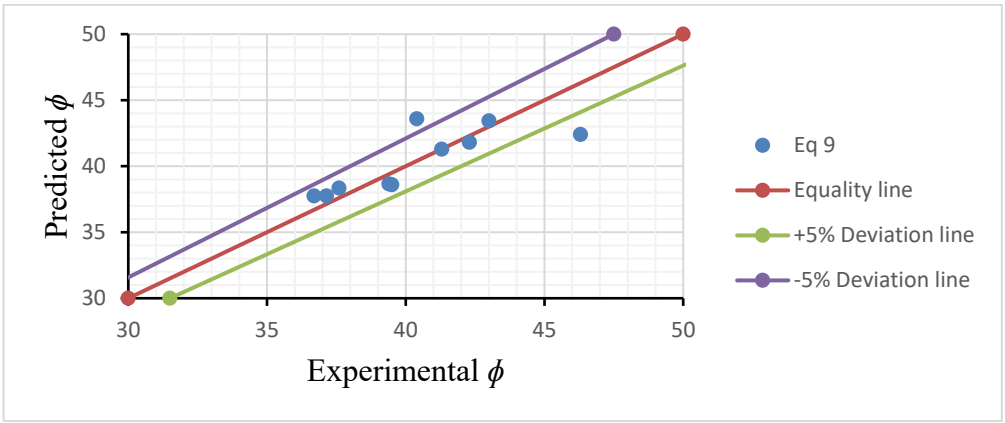

\

Fig. 12. Regression plot of actual and predicted values of friction angle according to Eq 9

3.5 Prediction of Internal Angle of Friction Based on Sieve Analysis and Modified Proctor Tests

Equations based on the sieve analysis parameters and the maximum dry density of the Modified Proctor test have been developed to relate the internal angle of friction to other parameters (Equations 10 to 14). Regression plots of actual values versus predicted friction angle values, based on Equation 12, can be seen in Figures 13-17. Regarding accuracy, Equation (12) has a relatively high R^2 value since it utilized multiple parameters like sand ratio, D_{10}, D_{30}, D_{50}, D_{60}, and maximum dry density from the modified proctor test. Equation 13 has the lowest R^2 value of the group.

$$\phi = -4.392 + 11.371\,D10 + 64.11\,D30 - 21.933\,D50 - 5.787\,D60 + 18.01\,\gamma_{max\,(MP)} \quad \text{Eq 10 } (R^2=0.64)$$

$$\phi = 57.37 - 0.196\,S - 0.013\,\gamma_{max\,(MP)} \quad \text{Eq 11 } (R^2=0.63)$$

$$\phi = 13.662 - 0.16\,S + 54.756\,D10 + 40.975\,D30 - 34.751\,D50 - 1.701\,D60 + 17.485\,\gamma_{max\,(MP)} \quad \text{Eq 12 } (R^2=0.79)$$

$$\phi = -6.564 + 0.425\,Cu + 10.832\,Cc + 17.358\gamma_{max\,(MP)} \quad \text{Eq 13 } (R^2=0.43)$$

$$\phi = 38.234 - 0.162\,S + 0.654\,Cu + 7.898\,Cc + 3.042\gamma_{max\,(MP)} \quad \text{Eq 14 } (R^2=0.73)$$

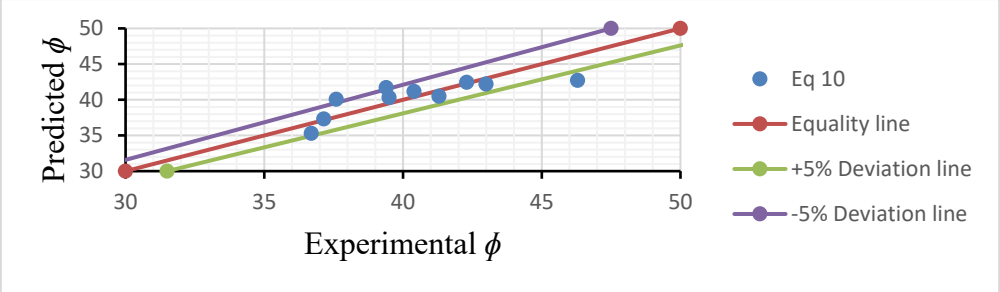

Fig. 13. Regression plot of actual and predicted values of friction angle according to Eq 10

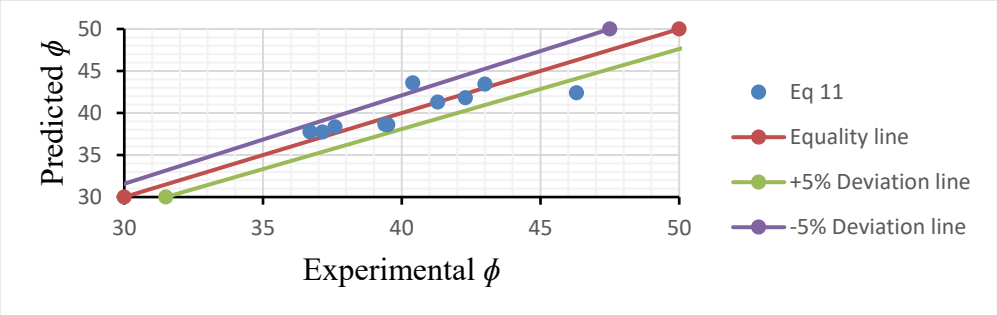

Fig. 14. Regression plot of actual and predicted values of friction angle according to Eq 11

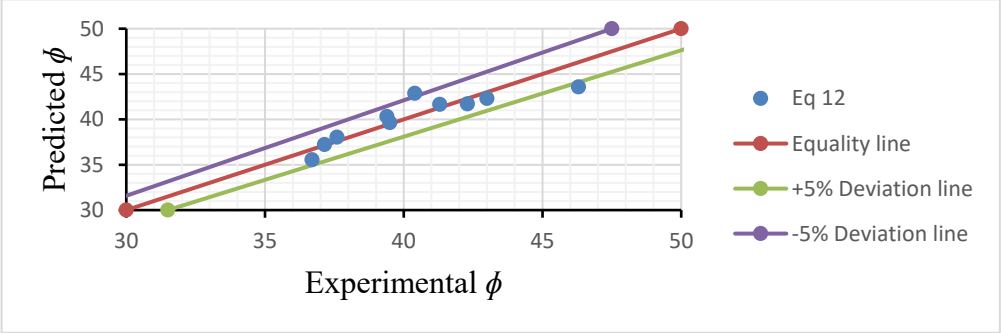

Fig. 15. Regression plot of actual and predicted values of friction angle according to Eq 12

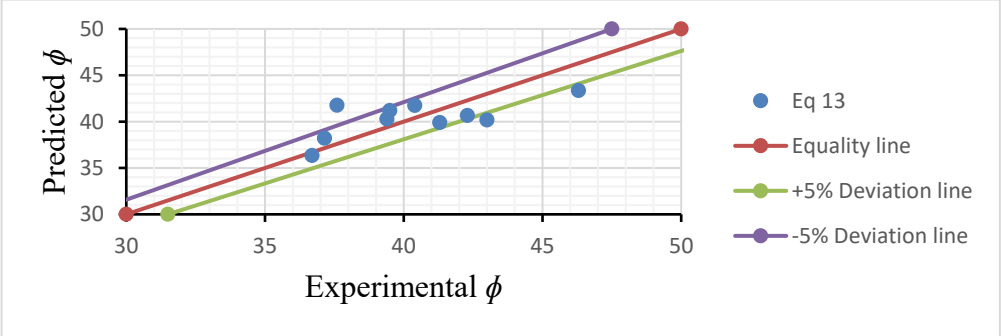

Fig. 16. Regression plot of actual and predicted values of friction angle according to Eq 13

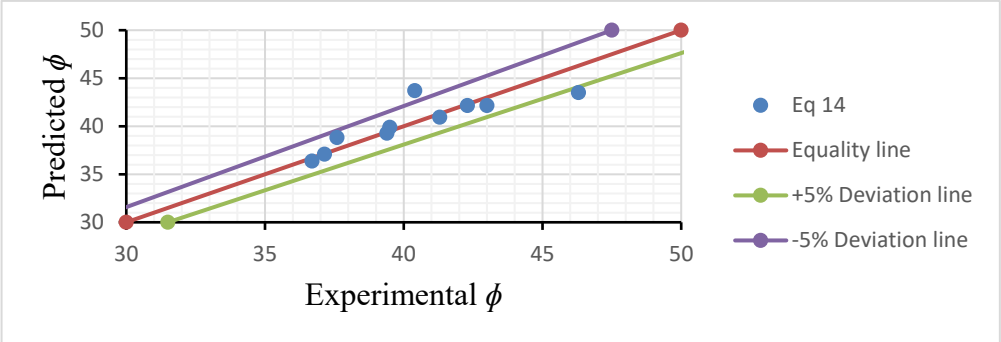

Fig. 17. Regression plot of actual and predicted values of friction angle according to Eq 14

4 Conclusions

In general, the effect of grain size distribution parameters on maximum dry density and internal angle of friction for coarse-grained soils can be significant. Thus, the following conclusions have been made:
(1) Maximum dry densities derived from standard and modified proctor compaction tests have a very strong relationship, with a high coefficient of determination ($R^2 = 0.94$).
(2) Maximum dry density (MP) and Cu and Cc have the same relationship as maximum dry density (MP) and D_{10}, D_{30}, D_{50}, and D_{60}.

(3) There is a best estimated relationship amongst maximum dry density (MP) and D10, D30, D50, D60, and maximum dry density (SP).
(4) There is satisfactory relationship between internal angle of friction and D_{10}, D_{30}, D_{50}, D_{60}, and sand ratio that is predictive.
(5) The highest estimate of internal angle of friction was determined by using D_{10}, D_{30}, D_{50}, D_{60}, sand ratio, and maximum dry density (MP) from the Modified Proctor test, with an R^2 value of 0.79. A weak estimate or lowest R^2 value of internal angle of friction was only made with Cu, Cc, and maximum dry density (MP).

References

1. Ren, X.C.; Lai, Y.M.; Zhang, F.Y.; Hu, K. Test method for determination of optimum moisture content of soil and maximum dry density. KSCE J. Civ. Eng. 2015, 19, 2061–2066.
2. Du, Y.J.; Hong, S.L.; Tao, W.; Hao, W. Experimental study on compaction characteristics of coarse-grained soil with discontinuous gradation. Chin. J. Geotech. Eng. 2019, 41, 2142–2148.
3. Miao, M.G.; Ning, L.; Chao, D.S.; Hui, C.Z.; Jubert, P. Experimental investigation of microscopic deformation mechanism of unsaturated compacted loess under hydraulic coupling conditions. Geotechnical. Mechanics. 2021, 42, 2437–2448.
4. Gang, W.; Yi, L.W.; Xing, W.; Ming, J.Z. Permeability variation of compacted clay during triaxial compression. Geomechanics 2020, 41, 32–38.
5. Rimbarngaye, A.; Mwero, J.N.; Ronoh, E.K. Effect of gum Arabic content on maximum dry density and optimum moisturcontent of laterite soil. Heliyon 2022, 8, 553.
6. Silva, A. V., Dantas Neto, S. A., and Souza Filho, F. A. (2016). A Simplified Method for Risk Assessment in Slope Stability Analysis of Earth Dams Using Fuzzy Numbers. Electronic Journal of Geotechnical Engineering, 21(10), PP. 3607-3624.
7. Mehran Karimpour-Fard, Sandro Machado, Amin Falamaki and Miriam F Carvalho, (2019). (Prediction of Compaction Characteristics of Soils from Index Test's Results), Iranian Journal of Science and Technology - Transactions of Civil Engineering 43 (11).
8. Bingyi Li, Zixuan You, Kaiwei Ni and Yuexiang Wang (2024), (Prediction of Soil Compaction Parameters Using Machine Learning Models), Applied. Sciences, 14, 2716.
9. Wang, H.L.; Yin, Z.Y. High performance prediction of soil compaction parameters using multi expression programming. Eng. Geol. 2020, 276, 105758.
10. Verma, G.; Kumar, B. Prediction of compaction parameters for fine-grained and coarse-grained soils: A review. Int. J. Geotech. Eng. 2020, 14, 970–977.
11. Farooq, K.; Khalid, U.; Mujtaba, H. Prediction of Compaction Characteristics of Fine-Grained Soils Using Consistency Limits. Arab. J. Sci. Eng. 2016, 41, 1319–1328.
12. Khuntia, S.; Mujtaba, H.; Patra, C.; Farooq, K.; Sivakugan, N.; Das, B.M. Prediction of compaction parameters of coarse grained soil using multivariate adaptive regression splines (MARS). Int. J. Geotech. Eng. 2015, 9, 79–88.
13. Hohn, A.V.; Leme, R.F.; Moura, T.E.; Llanque Ayala, G.R. Empirical models to predict compaction parameters for soils in the state of ceará, northeastern Brazil. Ingeniería e Investigación. 2022, 42.
14. Arama, Z.A.; Gençdal, H.B. Simple Regression Models to Estimate the Standard and Modified Proctor Characteristics of Specific Compacted Fine-Grained Soils. In Proceedings of the 7th World Congress on Civil, Structural, and Environmental Engineering, Istanbul, Turkey, 10–12 April 2022; pp. 1–9.
15. Khalid, U.; Rehman, Z.U. Evaluation of compaction parameters of fine-grained soils using standard and modified efforts. Int. J. Geo-Eng. 2018, 9, 15.
16. Omar, M., Shanableh, A., Basma, A., and Barakat, S. (2003). Compaction characteristics of granular soils in United Arab Emirates. Geotechnical and Geological Engineering, 21, 283–295. 10.1023/A:1024927719730.
17. Amanda V. Hohn, Rosiel F. Leme, Francisco C. da Silva Filho, Thales E. Moura and Grover Lianque A. "Empirical Models to Predict Compaction Parameters for Soil in the state of Ceara, Northeastern Brazil" INGENIERIA E NVESTIGACION, Volume 42, No. 1, April 2022, (https://doi.org/10.15446/ing.investig.v42n1.86328).

18. Moura, T. E. (2019). Modelos matematicos preditivos paraestimativa das propriedades de solos compactados [Undergraduate project, Federal University of Ceara]. Repositório Institucional UFC. http://www.repositorio.ufc.br/handle/riufc/49557.
19. Hassan Mujtaba, Khalid Farooq, Nagaratnam Sivakugan and Braja M. Das (2013). Correlation between gradational parameters and compaction characteristics of sandy soils. International Journal of Geotechnical Engineering, 7:4, 395-401.
20. for Testing and Materials (ASTM - D421) (2009), "Standard Practice for Dry Preparation of Soil Samples for Particle Size Analysis and Determination of Soil Constants" ASTM Book of Standards, Published in September.
21. American Society for Testing and Materials (ASTM D1557- 09) (2009), "Standard Test Methods for Laboratory Compaction Characteristics of Soil Using Modified Effort (56,000 ft-lbf/ft3 (2,700 kN-m/m^3))" ASTM Book of Standards, Published in October.
22. American Society for Testing and Materials (ASTM - D698) (2010), "Standard Test Methods for Laboratory Compaction Characteristics of Soil Using Modified Effort" west Conshohocken, PA, USA: ASTM International.
23. Egyptian Code for Soil Mechanics and Design and Executing the Foundations, 2001, part 3 (202/3), Egypt.